Fibers and Polymers 2000, Vol.1, No.1, 45-54

Impact Energy Absorption Mechanism of Largely Deformable Composites with Different Reinforcing Structures

Tae Jin Kang* and Cheol Kim

School of materials Science and Engineering, Seoul National University, Seoul 151-742, Korea
(Received September 1, 2000 ; Accepted September 15, 2000)

Abstract : Impact behaviors of the large deformable composites of Kevlar fiber reinforced composites of different preform structures have been investigated. An analytic tool was developed to characterize the impact behavior of the Kevlar composites. The image analysis technique, and deply technique were employed to develop energy balance equation under impact loading. An energy method was employed to establish the impact energy absorption mechanism of Kevlar multiaxial warp knitted composites. The total impact energy was classified into four categories including delamination energy, membrane energy, bending energy and rebounding energy under low velocity impact. Membrane and bending energy were calculated from the image analysis of the deformed shape of impacted specimen and delamination energy was calculated using the deplying technique. Also, the impact behavior of Kevlar composites under high velocity impact of full penetration of the composite specimen was studied. The energy absorption mechanisms under high velocity impact were modelled and the absorbed energy was classified into global deformation energy, shear-out energy, deformation energy and fiber breakage energy. The total energy obtained from the model corresponded reasonably well with the experimental results.

Introduction

A number of works have been reported in the fields of impact phenomena of fiber reinforced composite materials. Especially, the damage resistance and damage tolerance under impact loading are of the most importance of composite materials characteristics because they are often susceptible to impact. Low-velocity impact can introduce severe internal damages to composite structures and significantly reduce their load-carrying capacity[1-3]. Low-velocity impact damages may consist of matrix cracks, delaminations, and fiber breakage in a zone surrounding the impact point. Damage patterns are complicated such that the exact sequence of events involved and the size of the damage cannot yet be analytically predicted.

Delaminations are the main cause of reductions in mechanical properties of the laminate and usually cannot be detected by visual inspection except for in the case of translucent or transparent materials, thus, a lot of attention has been devoted to understanding how they develop during impact and how they propagate when subjected to further loading. After impact, many matrix cracks are present in a complicated pattern. It would be difficult to predict the final pattern of matrix cracks throughout the damaged region, but this would not be necessary as matrix cracks do not significantly contribute to reducing the residual properties of the laminate. However, many investigators believe that the entire damage process is initiated by matrix cracks, which then induce delaminations at ply interfaces[4-6].

*To whom correspondence should be addressed:
taekang@plaza.snu.ac.kr

The response of a laminated composite to an impact object depends on the impact parameters of the impactor and the material properties of the composites such as stacking sequence, interlaminar shear strength, tensile and flexural properties of the composites. When a foreign object impacted on the laminates, the impact energy was absorbed by the composite and damages such as delaminations, fiber breakage, and matrix cracks occurred in the composite structure. The carbon fiber reinforced composites or the glass fiber reinforced composites, which are susceptible to impact damage because of the brittle characteristics of the reinforced fibers, showed low impact energy absorption, and usually a complete penetration occurs by the impactor. The major energy absorption mechanism with the carbon fiber reinforced composite is fiber breakage mode. Damage mechanisms of ductile fiber reinforced composites such as Kevlar or Spectra fiber composites are quite different. The energy absorption is mainly due to the delamination and large deformation perpendicular to the impactor. Surface energy is needed to create newly delaminated surfaces, and strain energy is also required to deform reinforcing fibers in membrane deformation. Thus, the energy absorption mechanisms of ductile fiber reinforced composites are quite different form those of brittle fiber reinforced composites[7].

Furthermore, the energy absorption capabilities of brittle fiber composites are less than those of ductile fiber reinforced composites, thus, the Kevlar and Spectra fibers are widely used as an reinforcement fiber for the impact resistant composite materials. In consequence, understandings of the behavior of largely deformable composites such as Kevlar fiber reinforced composites under

impact condition are of critical importance in the field application.

When the impactor strikes the Kevlar plates, the plates absorbs impact energy solely by the elastic deformation if the incident impact energy is lower than a certain value. As the impact energy increases, matrix cracking occurs, and the delamination starts to propagates until the maximum delamination area has been reached. Thus, the dominant energy absorption mechanism is delamination mechanism in this stage. If the impact energy is higher than this stage, no additional energy absorption is possible by delamination growth. The Kevlar plates absorbs additional impact energy by the inelastic deformation of the plates, including bending and membrane deformations called as bulging. If the impact energy is above this level, when the impactor velocity is high and the contact time is not enough to transfer impact waves induced by the impactor, then the localized damage including fiber breakage and delamination occurs.

Delamination, fiber breakage, inelastic deformation absorb impact energy, but it is not clear which one is dominant at each stage. It is not known how the relative energy absorption changes with increasing incident impact energy. It is not known whether the delamination still absorbs significant energy for the case of perforation, or if it can be neglected compared to the energy absorbed in fiber breakage. The main object of this paper is to fully quantify the relationship between the damage mechanisms and energy absorption under low and high velocity impacts.

Energy Balance Equation

To analyze the impact damage mechanism of a Kevlar composite, it is assumed that no fiber breakage occurs under low level of impact energy. When the impactor strikes the specimen surface, the given impact energy by the impactor can be classified into two quantities. One is the elastic energy which is stored elastically in the specimen and transferred back to the impactor. Another is the absorbed energy which is the sum of the absorbed energy in the specimen by its damage initiation and propagation, and the energy absorbed by the impact system in vibration, heat, inelastic behavior of the impactor or supports.

Thus, the following relationship holds under low velocity, low energy impacts.

$$E_{total} = E_{reb} + E_{abs} \tag{1}$$

where E_{reb} : rebounded energy,
E_{abs} : absorbed energy,
E_{total} : total energy

Furthermore, the absorbed energy can be divided into two classes; one is E_{ab}, which is absorbed by the specimen while the other is E_{sys} which is absorbed by the testing system itself. The total energy absorbed by the specimen has three components E_{mb}, E_{bd} and E_{del}, which are respectively, membrane energy, bending energy, and energy absorbed by the creation of damages in the matrix. For a ductile Kevlar composites, we assumed that fiber breakage did not occur, therefore, the terms which related to fiber breakage were ignored, and delamination energy E_{del}, dominated. Thus, the resultant equation for the impact energy is given as

$$E_{total} = E_{reb} + E_{mb} + E_{bd} + E_{del} \tag{2}$$

Triangular elements were used to calculate the membrane and bending energy. Membrane strain energy expression and its derivative with respect to coordinate is given as :

$$E_m = \frac{1}{2}\{\varepsilon\}[C_m]\{\varepsilon\}S \tag{3}$$

where $[C_m]$ is a tensile property matrix

Bending strain energy can be expressed as follows using the coordinate information of the three elements neighboring the current element, the bending energy term can be expressed as :

$$E_B = \frac{1}{2}Tr([P][C_b]^t[P])S \tag{4}$$

In this study, delamination energy E_{del} was obtained by a damage area analysis. If a composite laminate was impacted by an object, the delamination initiated below the impacted area and broad delaminations could form with the increase of impact energy. Additionally, matrix cracking could have occurred, but many researchers reported that matrix cracking plays an important role at the onset of delamination. No attempts were made to divide delamination and matrix cracking, since matrix cracking is always associated with delamination and the ratio of matrix cracking area and delamination area is constant for a given system, or the energy absorption by matrix cracking is often negligible. If the fracture toughness of the laminate is known, the energy needed to delaminate a given area can be calculated. The impact fracture toughness i.e., the unit energy needed to delaminate a unit area by impact, can be measured from the relationships of impact energy and delaminated area. To obtain the precise estimation of delaminated area, the deply technique was adapted as it will be described later. Once the impact fracture toughness has been measured, the following equation is applicable.

$$E_{del} = K \cdot \sum_{i=1}^{n-1} A_i \tag{5}$$

where E_{del} : delamination energy,
K : fracture toughness under impact,
A_i : delaminated area in the i^{th} layer,
n : number of plies

Finally, the total absorbed impact energy by impact loading is the sum of the delamination energy, bending energy and membrane energy.

Experimental

Materials

Kevlar 29 fiber was used for reinforcement as well as for stitch fibers. Three kinds of preforms were used. One is multiaxial warp knitted preform(MWK) and another is woven fabric as well as unidirectional angle ply were stacked and consolidated with epoxy resin. Multiaxial warp knitted preforms can be called 'high performance multiaxial warp knitted preforms because a Kevlar fiber was used as stitch yarns. This multiaxial warp knitted fabric consisted of insertion yarns of four directions(warp and fill, bias yarns of +45/-45) with two types of stitches, i.e., tricot and chain stitches. And this multiaxial warp knitted fabric is defined as QTC(quadriaxial insertion yarn/ tricot/chain stitch) preform. The unidirectional laminate was stacked with a sequence of $[(0/45/-45/90)]_s$. For woven laminates, 8 plies of fabric having a density of 21 count per inch for warp and fill were stacked to obtain a 4 mm thickness of composites. Thin teflon strips (<5 μm) were inserted between each plies to make ease of deplying. Laminates were press-claved at 120°C for 90 min at 5 MPa pressure, then cooled to room temperature.

All impact specimens were prepared to have 4 mm thicknesses and 0.53-0.61 fiber volume fractions.

Tests and Specimens

The in-plane Young's modulus as well as the in-plane Poisson's ratio were determined by a tensile test, following ASTM D 638 M. An extensometer was also attached with respect to the center line of the specimen, having a gage length of 1 in. Shear properties of the composites were obtained using a Iosipescu shear test fixture, which could offer a pure shear stress on the neutral plane of the test specimen. A schematic diagram of a Iosipescu test fixture is shown in Figure 1. Bending properties were obtained by ASTM D 790a where a four point bending test method was used. Span-depth ratio was 16:1, while the crosshead speed was fixed at 1 mm/mim.

Impact test

The instrumented impact test equipment used in this study was a ITR-2000 impact tester. The general features of the testing apparatus are shown in Figure 1. The material specimen is a flat plate, approximately 127-mm(5-in.)

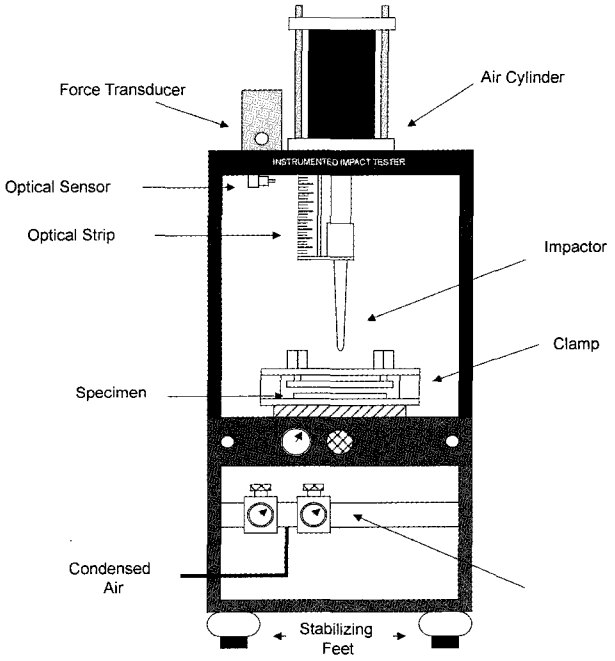

Figure 1. Instrumented impact tester.

square, which is securely clamped over a 101 mm(4 in.)-diameter annular anvil. The test consists of complete penetration of the specimen by a 12.5 mm(1/2-in.)-diameter hemisphere probe which is guided through the center of the annulus under conditions of near constant velocity. It is possible, with tough materials, to have the undesirable condition of large velocity variations of the probe during penetration.

The probe is equipped with transducers for measuring velocity and the load interaction between the probe and specimen. Photoelectric sensors are used to start and stop data acquisition. Three thousand load data points are collected during the 101 mm(4 in.) of probe travel which is considered to be the impact event. The velocity and load transducers provide complete profiles of the deformation response of specimen from initial impact to final penetration.

A thick composite laminate was first impacted at low impact energy levels and a penetrant was injected during the deplying process to enhance the image resolution of the delaminated areas. After the injection of penetrant, the laminates were deplied and the damaged area induced by the impact loading were measured. In order to measure fracture toughness correctly, the impact specimens to have enough thickness and the incident impact energy level had to be kept low to avoid involving vertical deformations and indentations.

In order to evaluate impact properties of the thin composite laminate specimen, the following steps were performed. Before impact, a number of points were

printed on the back surface of the laminates to obtain a 3-dimensional deformed shape after impact loading, as previously described[8-10]. Impacts were inflicted on the laminates using an instrumented impact tester. The diameter of the impact tip was 12.7 mm while the 100 × 100 mm size specimens were clamped by an aluminum fixture by a pneumatic pressure of 600 kPa. Impact energy was varied by altering the initial velocity of the impactor. Once impacted, the image of the back surface of the impacted specimen was captured and analyzed to obtain the deformed coordinate.

Results and Discussion

Responses under Impact Loading

A photograph of the cross-sectional area of the impacted specimen is shown in Figure 2. Broad delamination and large deformation can be found in the entire region of specimen (a), which was impacted at 7.0 m/s initial velocity. Thus, it is reasonable to assume that the main energy absorption mechanisms are delamination and global deformation including membrane and bending deformations because no fiber breakage can be found in figure (b), energy absorption mechanisms under high velocity impact are fiber breakage, delamination and so called, shear out process and global deformation. The principle damage is apparently fiber failure, as a substantial bundle has been detached from the matrix and pushed along the direction of the striker motion. The shape of the damaged region depends upon the weave and lay-up of the specimen. A woven laminate showed a square-shaped damage zone on the distal side with an extent of 1.5-2 times of the impactor diameter, while the QTC composite, resulted in a circular pattern.

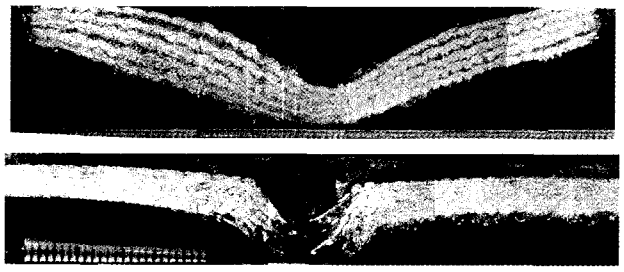

Figure 2. Cross-section of impacted specimens (upper : low velocity, under : high velocity).

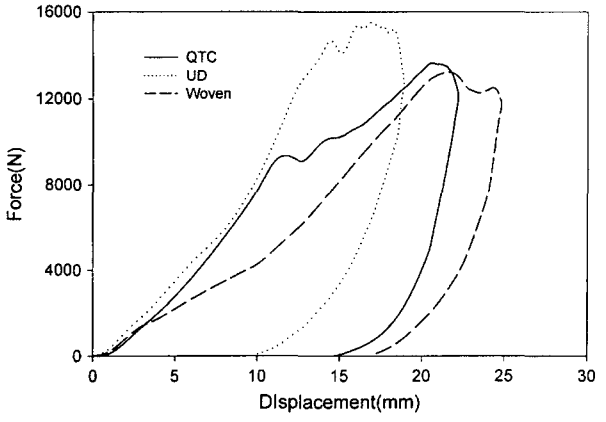

Figure 3. Force-displacement curves under impact loading (7.0 m/s with 6.5 kg).

Force-displacement curves under impact loading are shown in Figure 3 Since the impact velocity was not high enough to infiltrate full penetration of the composite, non-perforated impact occurred at 7.0 m/s velocity, while all the specimens were perforated at 11.0 m/s initial velocity. From this figure, it is clear that the unidirectional laminates showed more elastic features than other specimens since the unidirectional laminates responded more quickly upon impact loading at low impact velocity. Unidirectional laminates have much higher initiation energy than the propagation energy while other specimens showed otherwise. Both woven and QTC multiaxial warp knitted preform composites showed more ductile features than the unidirectional laminate. At high impact velocity, the force-displacement curves showed similar tendency.

The impact time could be measured during the impact test and varied within the range of 6.4-7.1 ms for low velocity impact while 3.6-4.1 ms for high velocity impact. From the experimental data obtained from the force transducer. Duration of impact phenomena of MWK fabric reinforced composites were longer than that of UD and woven laminated composites.

The variation of total energy dissipated during impact are shown in Figure 4. The energy diagram includes both the energy to induce damage as well as the energy dissipated via recoverable deformation and other secondary mechanisms such as the delamination energy, bending and membrane energy, etc.

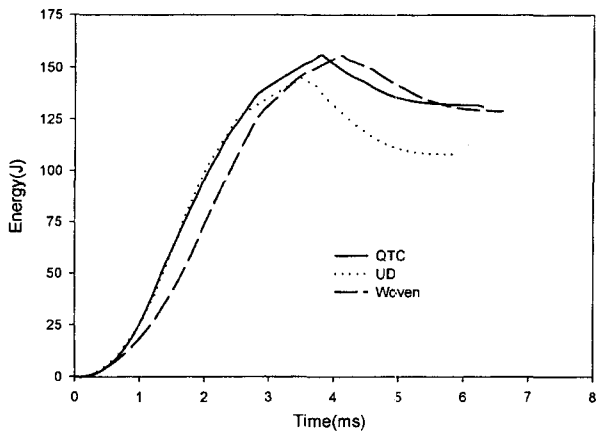

Figure 4. The variation of total energy dissipated during impact.

Delamination Area and Energy Level

For a woven laminate, delamination initiated at the center of impact, and propagated to the directions of warp and fill directions. Due to the existence of warp and fill reinforcements, impact damages which initiated by matrix cracks were propagated along them. For unidirectional laminates which were fabricated up to 24 plies, the direction of the delaminations always followed the direction of the reinforced fibers in the lower ply of each interface. For example, in the -45°/+45° interface, delamination occurred in the +45° direction. And this phenomena coincides with the results by Guynn and O'Brien[11], who observed that the delaminations always followed the matrix cracks in the back ply of each unique interface.

All the captured images of delaminated area are stored with 640×480 pixels. Five identical specimens were impacted, of which three of each five specimens have deplied to obtain the delaminated area images. Data shows that limits of delamination by impact exist. Since the impact specimen was clamped by an impact fixture as mentioned earlier, it is clear that delaminated areas have an upper limit extending up to the inner area of the clamp. Delaminated patterns of the QTC and woven specimen are shown in Figure 5. The delaminated areas induced by the impact loading for the laminated composites of various types of preforms are shown in Figure 6 at various impact energy levels.

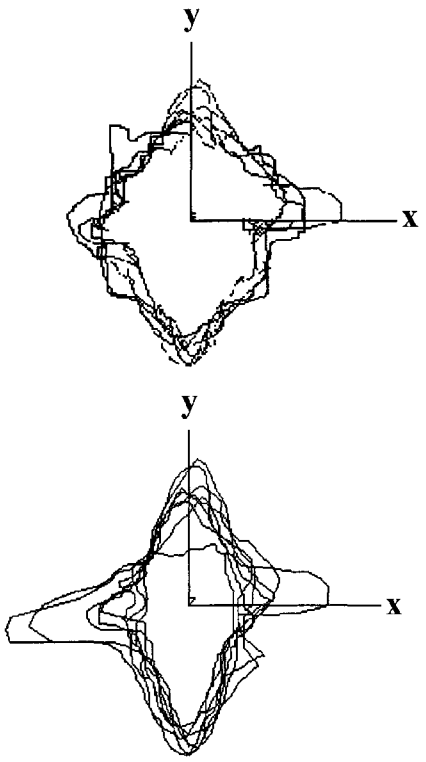

Figure 5. Delaminated patterns of the QTC and woven specimen (upper : QTC, under : woven, both impacted at 7.0 m/d initial velocity).

The absorbed energy of Figure 6 indicates the total absorbed impact energy including membrane, bending and delamination energy. Since the initial slopes of Figure 6 implies the delaminated area by unit impact energy, impact fracture toughness can be obtained by inverting the slopes. As shown in Figure 7, the fracture toughness of the multiaxial warp knitted composite is higher than that of the woven laminate or unidirectional laminate composites. Impact fracture toughness values were 3.84 kJ/m^2 for the QTC composites, and 1.22 and 1.39 kJ/m^2 for the unidirectional laminate and woven laminate, respectively. At the same level of given impact energy, multiaxial warp knitted fabric composites, especially QTC composites showed the smallest damaged area. This means that the QTC composite is capable of absorbing higher impact energy and constraining the damaged area to a relatively small region.

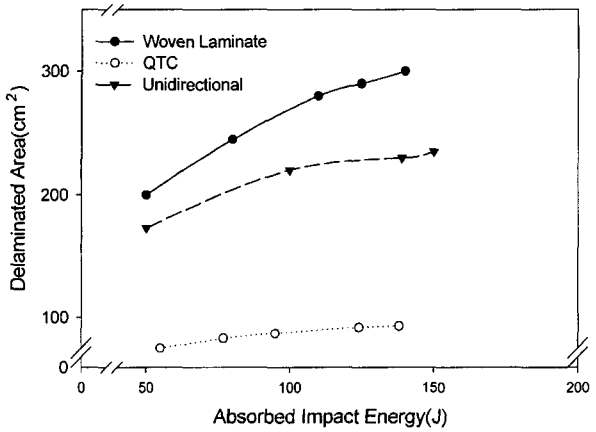

Figure 6. Delaminated area-absorbed energy relations of various composites.

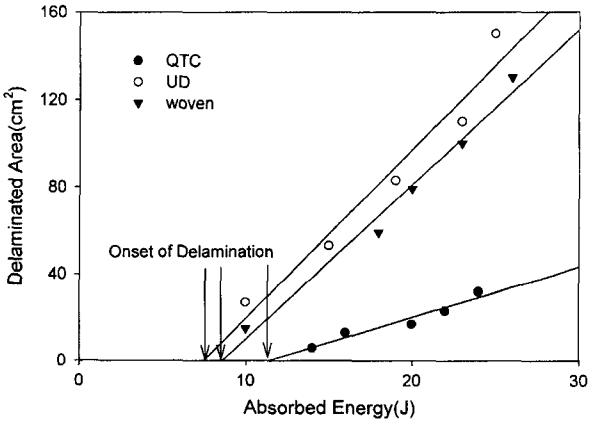

Figure 7. Impact fracture toughness.

The interceptions of the lines on the energy axis indicate minimum incident energy levels needed to start the onset of the delamination. For the QTC specimen, 11.5 J of impact energy were necessary to initiate delamination. However, the woven laminates and unidirectional laminates the impact energy was about 7-8 J. These results coincide well with other test results, since the QTC showed higher interlaminar shear strength and thus higher energy was needed to initiate interlaminar impact damage such as delaminations. Conventionally it is believed that perforation takes place above this level of impact. Additional energy absorption is possible by means of fiber fracture. In contrast to glass composites, Kevlar composites can absorb additional impact energy by the global deformation as well as fiber fracture mechanism. Thus, absorbed energy-delaminated area relationship of Kevlar composites is different from that of glass composite.

Membrane and Bending Energy

Using the image analysis method, the membrane and bending energy were calculated from the impact induced deformed shape of the impacted specimen. The reconstructed 3-D images are shown in Figure 8. With the coordinate information of the deformed specimen from the image analysis, the membrane and bending energies were calculated. Coordinates of transitional steps between non-deformed and deformed specimens were generated by linear interpolation. Velocity profiles of the impactor were used to calculate the time scale for the transitional steps.

Now, all the energy absorbed by each mechanism of E_{reb}, E_{del}, E_{mb}, E_{bd} have been calculated. The impact energy is divided into three major parts at low velocity impact: the rebounding energy part, measured from energy impact data; the delamination energy part, which needed to initiate and propagate delaminated surface, and which was calculated by impact fracture toughness and delaminated area measured by the deply technique; deformation energy which were computed using images of deformed specimens and material properties.

For high velocity impact, the image analysis technique could not be used because of the relatively small global deformation of the specimen. Thus, the energy absorbed by global deformation under high velocity impact were obtained by static indentation tests.

A static indentation test was performed to the undamaged specimen until the same global deformation was achieved. Since additional delamination could occur during this static test, delamination energy was calculated by deply method as proposed in an earlier section. Thus, the energy absorbed by global deformation can be calculated.

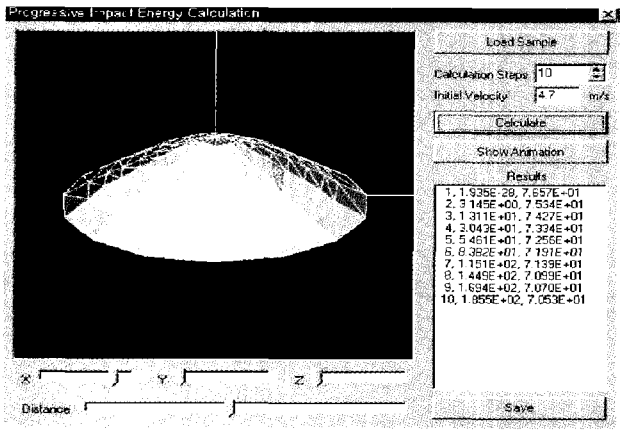

Figure 8. Reconstructed 3-D images and example of energy calculation.

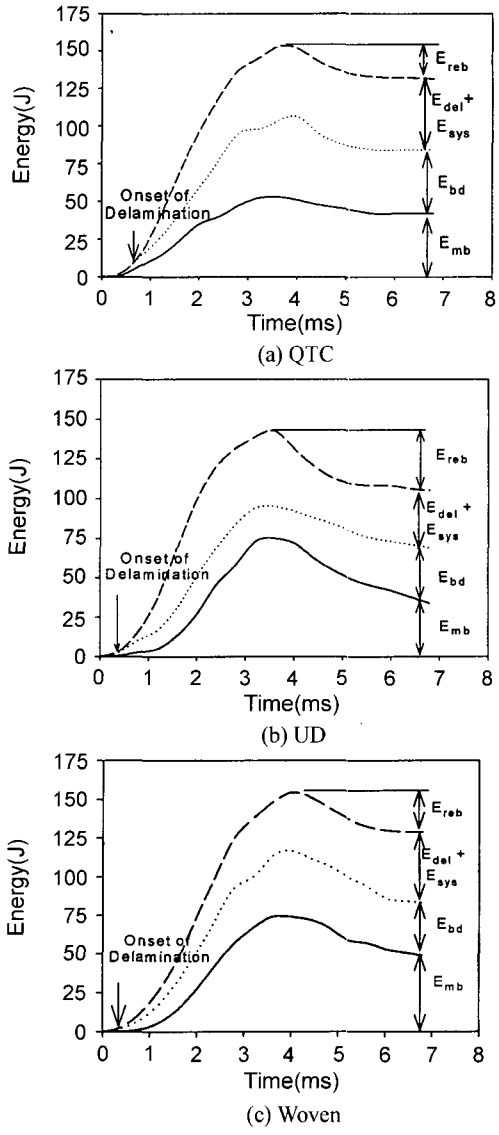

Figure 9. Breakdowns of energy absorption under low velocity impact (upper : QTC, middle : UD, lower : woven).

Energy absorption by shear-out was estimated by first determining the transverse fracture energy of the material. In order to obtain this, an out of plane shear test was performed by the Iosipescu shear fixture. This technique yielded values of 104 kJ/m^2 for woven laminates. Consequently, the shear-put energy was calculated by multiplying this fracture energy by the area of shear zone. Energy dissipated in delamination was estimated by multiplying the delamination area with the impact fracture toughness obtained in an earlier section on low velocity impact. Energy absorbed by fiber breakage was calculated by examining broken fiber width in each ply.

Thus, the total energy required to perforate the Kevlar composites investigated in this study was then determined by adding the estimated energies associated with global deformation, shear-out, delamination and fiber breakage[12].

Energy Absorption Mechanism under Low Velocity Impact

The breakdown of absorbed energy under low velocity impact is shown with different mechanisms of energy absorption in Figure 9.

The total impact energy is the sum of the component energy of E_{del}, E_{bd}, E_{mb} and E_{reb}. We did not consider the E_{sys} term nor the energy absorbed by fiber breakage since the incident energy was not sufficient enough to cause the fiber breakage. The gaps between incident energy and the summation of membrane and bending energy are sub-summations of E_{sys} and the energy absorbed by fiber damage or delamination. Delamination energy can also obtained by multiplying the delaminated area and impact fracture toughness. The delamination energies calculated in this way was 36 J for QTC, 29 J and 42 J for unidirectional laminates and woven laminates, respectively. Note that all the delamination energies are lower than the gaps in the figures. From Figure 11, sub summation of delamination energy, E_{sys} and energy absorbed by fiber breakage are 48 J, 36 J and 46 J, respectively. These results indicate that the energy absorbed by other mechanisms remain small compared with the energy absorbed by the major energy absorption mechanisms such as delamination and global deformation.

As reported in the previous section, the impact fracture toughness of multiaxial warp knitted composites are significantly improved by the existence of through-the-thickness stitched loops. Although the fracture toughness was improved, the total energy absorbed by delamination was not increased as much since the delamination area was drastically reduced with the multiaxial warp knitted composites. Woven laminate, which had the lowest impact fracture toughness, showed much greater delamination energy absorption because of the broad extent of delamination.

For non-perforating impact tests the incident energy was fully transferred to the specimen at the point of maximum impactor displacement. After the maximum displacement, the specimen transfer elastically stored impact energy back to the rebounding impactor. The ratio of rebounded energy to stored energy could be a parameter of elastic/plastic properties. Ratios of rebounded energy to stored energy were 0.17 for QTC multiaxial warp knitted composites, 0.35 and 0.14 for unidirectional laminate and woven laminate, respectively. This tendency is similar to the results from force-displacement relationships.

The onsets of delamination were also shown in the above figures. The multiaxial warp knitted composites showed retarded delamination onset. Delamination initiated at 0.7 ms with 11 J of impact energy for QTC specimens, while 0.3-0.4 ms and 5-6 J were necessary for the unidirectional laminate and woven laminates, respectively. The results correspond well with the other test results since the fracture toughness of the former specimen is much higher than those of the latter two specimens.

For the QTC composites, the main modes of impact energy absorption were deformation, bending and membrane mechanisms from the beginning of impact loading until maximum displacement was reached. After maximum displacement had been reached, the impact energy stored by bending and membrane deformation was transferred back to the impactor. Unidirectional laminate showed greater elastic characteristics than other specimens, such as higher rebounding energy, lower displacement, and shorter total impact time. Woven laminates showed less elastic features than any other specimen. It showed higher deformation, longest impact time, smallest rebounded energy. It absorbed more energy by means of membrane energy mechanism than other mechanism, thus resulting in relatively small bending energy absorption although the deformation is large since the bending stiffness is lower than multiaxial warp knitted composites.

Two kinds of additional experiments were performed to verify the energy absorption mechanism. One was a delamination simulated impact test which was done by impacting a composite plate having thin Teflon films in each interply. The other was a deformation restricted impact test in which global deformation of the impacted specimen was restricted by the clamping fixture which has a smaller diameter.

Delamination simulated specimens were made by the insertion of thin Teflon films in each interply of woven laminate composites. A thin Teflon film(<5 μm) of 40 mm radius was inserted in each interply to simulate delamination. All other parameters including cure temperature and fiber volume fraction were unchanged. Restriction of global deformation was done by the fixture of a smaller diameter.

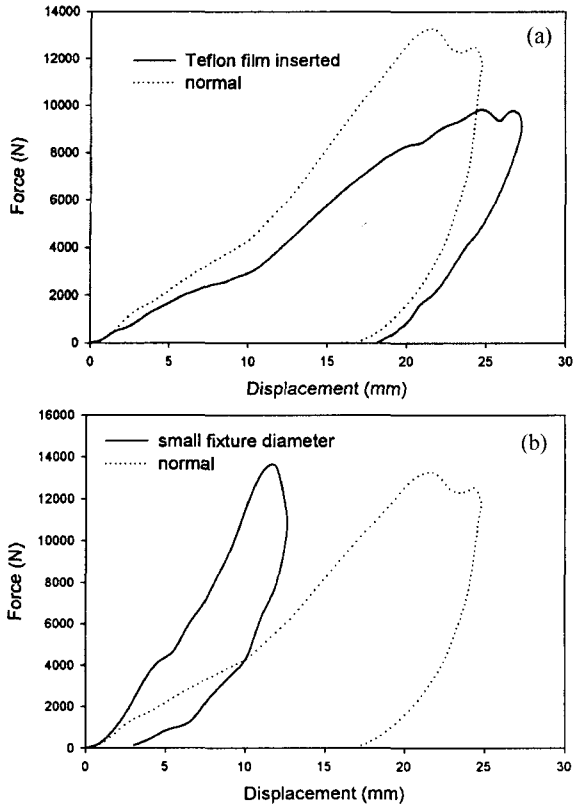

Figure 10. Effect of delamination and global deformation on the energy absorption under low velocity impact ; (a) force-displacement curves of normal/delaminated specimens, (b) force-displacement curves of normal/restrained specimens.

The resultant force-displacement curves for a 8 ply laminate with an embedded 80 mm diameter delamination and that of fully laminated plates when impacted by a 12.7 mm hemispherically tipped impactor are presented in Figure 10.

The delaminated specimen has a lower initial slope, and slightly lower peak load but slightly increased deformation. At the initiation of rebounding, up to the point of maximum deformation, the delamination simulated specimen absorbed approximately 71% of the homogeneous laminate energy and exhibit 74% of its peak load. These figures provide an idea of the effect of delamination.

According to the results of the above energy calculation, the woven laminate absorbs 33% of its maximum energy absorption by delamination mechanism. Results of the delamination simulated specimen showed good correspondence well with the previous calculated result.

Also, the effect of restraint on global deformation and delamination are shown in Figure 10. The peak load for the two cases are about the same, but the restrained system exhibits a much lower deflection both at the maximum load and at the end of the test. Thus, the energy absorption of restrained specimen was up to 36% of unrestrained specimen. Also, for the restrained specimen, energy absorption by delamination had reduced. The energy absorbed by delamination was up to 79% of unrestrained specimen, 33.2 J. But this quantity is not sufficient to explain the reduction of total absorbed energy. Thus, it is reasonable to consider that the reduction of energy absorption of restrained specimen is mainly due to the reduction of global deformation.

Energy Absorption Mechanism under High Velocity Impact

As discussed earlier, energy absorption mechanisms which are available in composite materials are fiber breakage, membrane deformation, bending deformation and delamination. For low velocity impacts, bending deformation and delamination are the major energy absorption mechanisms. At energies above the threshold, the fracture zone are generally conical in shape with the overall area of damage increasing towards the lower surface of the composite. This type of conical-shaped fes, as well as in a number of metals.

In high velocity impacts, at the perforation threshold energy, the spherical tipped impactor generally make a conically shaped shear plug as it penetrates the impact specimen and energy dissipates during this process. Thus the energy absorption mechanisms under high velocity impacts can be classified as global deformation, fiber breakage, delamination and shear-out.

The total energy required to perforate the impacted specimens are calculated and compared with those of experimental results in Table 1 (A) is the experimental value. The calculated energies by each of the energy

Table 1. Comparison of calculated and experimental results of the energy absorption under high velocity impact

(unit: J, standard deviation in bracket)

Specimen	(A) Predicted	(B) Experimental(S.D)	(C) Calculated (J)				
			Total	Fiber breakage	Global deformation	Delamination	Shear out
BTC	176	182(5.08)	172(5.3)	91.5	14.2	24.6	42.7
QTC	184	188(6.85)	177(7.1)	94	10.3	22.6	50.1
UD	154	145(8.59)	137(9.1)	72	8.3	20.2	37.1
Woven	188	203(9.1)	182(7.4)	100	15.6	26.3	40.9

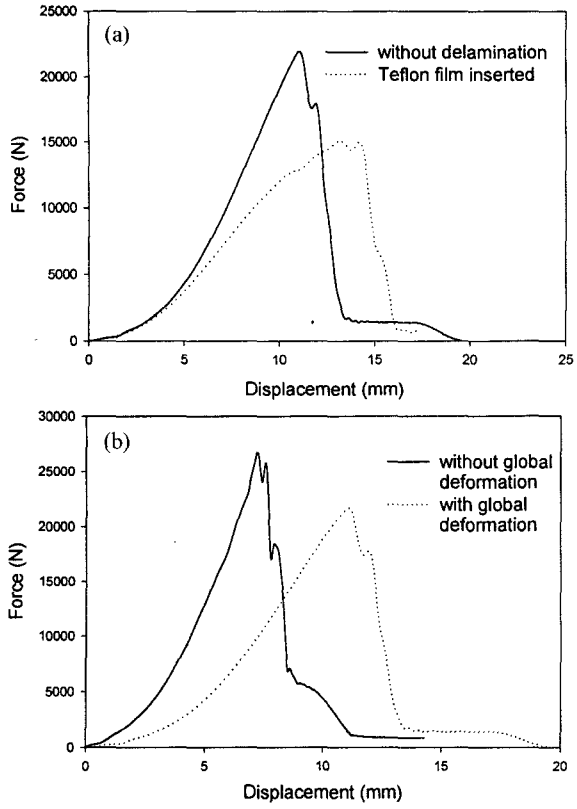

Figure 11. Effect of delamination and global deformation on the energy absorption under high velocity impact ; (a) force-displacement curves of normal/delaminated specimens, (b) force-displacement curves of normal/restrained specimens.

absorption mechanisms are shown in column (B).

As shown in this table, the experimental values have slightly higher than the predicted energy level, since excess energy absorbed by other mechanisms such as vibration and noise are neglected. Energy absorption in UD angle ply laminates showed the lowest values, since the fiber breakage energy of this specimen showed the lowest value.

QTC composite specimen showed higher shear out energies than those of UD or woven laminates. An additional impact test similar to tests done with low velocity impacts has been performed. The results are shown in Figure 11 for the delamination simulated and restrained tests, respectively. All the test configurations are the same as the low velocity impact, except for the impact velocity.

From these figures it is clear that the delamination and global deformation have little effect on the energy absorption. The results are reasonable because their contribution to energy absorption is relatively small compared with the energy absorption by fiber breakage and shear out processes.

The energy absorption of the delamination simulated specimen decreased about 4% of the undelaminated specimen, while the restrained specimen showed a 12% decrease in energy absorption. All of these results coincide well with the results in the previous section.

In contrast to the trends observed in the low velocity impact, the effects of varying the fixture diameter does not appear to vary the perforation energy significantly at this impact energy level. The strong geometric dependency observed in the low velocity impact may be attributed to the global deformation. Under high velocity impact conditions where the contact time between the impactor and the target specimen is very short, it appears that the total energy absorbing capability of the specimen is not utilized, and the impactor indeces a very localized form of target response. As a result, varying the specimen geometry does not show any significant effect on the energy absorption, and the extent of damage incurred. This reasoning is also supported by the associated delamination area analysis, where no significant variation in the total delaminated area was noticed.

Conclusions

Impact properties of largely deformable composites of Kevlar fiber reinforced composites with different reinforcing structure have been investigated. An analytic tool was also developed to characterize the impact behavior of composites. The image analysis and deply techniques were employed and energy balance equation was established.

An energy approach was employed to study the impact behavior and impact energy absorption mechanisms of largely deformable composites under low and high velocity impacts.

The multiaxial warp knitted composite showed higher impact fracture durability and bending properties, resulting in increased delamination and bending energy compared with unidirectional laminate. For woven laminates, since the delaminated area of the woven laminates was much larger than that of multiaxial warp knitted composites, it absorbed slightly more energy in delamination mode although the impact fracture toughness of the woven laminate was much smaller than that of the multiaxial warp knitted composites.

The onset of delamination was retarded in multiaxial warp knitted composites because of higher impact fracture durability than those of unidirectional laminate or woven composites. The multiaxial warp knitted fabric composites showed reduced delaminated areas at the same incident energy level because the energy absorbed by delamination was larger and not much lower than that of woven laminate with the presence of stitched loop fibers. This means that the multiaxial warp knitted composite has the capability of absorbing high impact energy while constraining the damaged area into a relatively small region.

References

1. F. Scardino, "Comp. Mat. Series", (R. Pipes Ed.)s, Vol. 6, pp. 22-24, Elsevier, NY, 1989.
2. A. Kinsey, D. E. Saunders, and C. Soutis, *Composites*, **26**, 661 (1995).
3. G. Clark, *Composites*, **20**, 209 (1989).
4. D. Delfosse and A. Poursartip, *Composites*, **28A**, 647 (1997).
5. C. C. Jr. Poe, "Simulated impact damage in a thick graphite/epoxy laminate using spherical indenters", NASA TM-100539, NASA Langley Research Center, VA, 1988.
6. C. T. Sun and J. E. Grady, *Composite Science and Technology*, **31**, 55 (1988).
7. S. Abrate, *Applied Mechanics Reviews*, **44**(4), 155-190 (1991).
8. W. J. Cantwell and J. Morton, *Composites*, **22**(5), 347 (1991).
9. R. Ayres, E. G. Brewer, and S. W. Holland, *Transactions SAE*, **88**, 2630 (1979).
10. A. Miyoshi, A. Yoshioka, and G. Yagawa, *Engineerings with Computers*, **3**, 149 (1988).
11. J. H. Vogel and D. Lee, *Journal of Materials Shaping Technology*, **6**, 205 (1989).
12. E. G. Gyunn and T. K. Obrien, "Proc. 26th Structures, Structural Dynamics, Material Conf.", Orlando, FL, April, 187 (1985).
13. G. Zhu, W. Goldsmith, and C. Dharan, *Int. J. Solids Structures*, **29**, 399 (1992).